Influence of Temperature and Potential on the Electrochemical Dissolution of Galena in HNO₃ at pH 2.0

Qingyou Liu[1], Guoheng Jin[1,2], Kai Zheng[1,2], Xiaoying Wen[1], Heping Li[1,*]

[1] Institute of Geochemistry, Chinese Academy of Sciences, Guiyang 550002, China
[2] University of Chinese Academy of Sciences, Beijing, 100039, China
[*]E-mail: liheping123@yahoo.com

We investigated the influence of temperature and add potential on the electrochemical dissolution of galena in HNO_3 at pH 2.0. Potentiodynamic curves showed galena different electrochemical reaction states. From OCP to 160 mV (vs. saturated calomel electrode) galena was passivated with S^0, 160-320 mV was active dissolution, S^0 transformed into $S_2O_3^{2-}$, and potential above 320 mV was double-inductive area, $S_2O_3^{2-}$ transformed into SO_4^{2-}. High temperature accelerates galena electrochemical dissolution, when temperature increases from 25 °C to 40 °C, and then to 55 °C, the promotion efficiency is 233.33% and 322.22%, respectively. Electrochemical impedance spectroscopy (EIS) results are well in agreement with the three potential regions, and reveal the cause that high temperature accelerates galena electrochemical due to decreases charge transform resistance and passive resistance at passive potential area. These experimental results will give experimental basis for galena weathering explains and hydrometallurgy applied.

1. INTRODUCTION

Galena (PbS) is the important sulphide lead mineral and one of the most intensively studied sulfide mineral due to its importance as the main source of lead [1]. In Nature, galena can easily be weathering either as natural minerals or as wasted residues, contributing significantly to the enrichment of heavy metal ions (such as Zn, As, Cd, and so on) in the surrounding environment, and even to human body through the food chain, leading to a range of health problems and increase the risk of cancer [2].

There is no denying galena oxidization is an electrochemical process in nature [3]. In air condition, galena oxidization is a very complicated progress. Previous studies indicated that PbS

oxidization involving unequal amounts of Pb and S species [4-6]. In solution, the anodic dissolution process of galena is seriously affected by pH. In acid system, generally, the anodic dissolution process was expressed as [7]: $PbS \rightarrow Pb^{2+} + S^0 + 2e^-$. In neutral or alkaline solution, galena oxidization produce changes more complicate basic lead thiosulphate, Lead thiosulphate [8, 9] or lead sulphate and sulfur [10] were all confirmed. However, the exact structural and chemical identity of the species rendering sulfide surfaces hydrophobic under moderate oxidizing conditions in solution is still under debate. Especially, to the passive-active area, applied different anodic potentials could cause galena lie in passive or active state and occur different oxidation state of sulfur. Nava et al. [11] investigated the oxidation of galena in perchlorate medium at pH 0, they revealed that for $E < 0.6$ V vs. saturated calomel electrode (SCE), elemental sulfur and Pb (II) were produced, whereas for $E > 0.6$ V vs. SCE, thiosulfate and sulfate ions were produced. Gonzalez et al. [12] studied the influence of chloride ions on the electrochemical oxidation of galena concentrate in perchlorate medium at pH 2.0, that in perchlorate solutions the galena is oxidized forming several products dependent on the applied potential. When the potential is below to 0.54 V vs SCE, Pb (II) and elementary sulfur are formed. Galena oxidation to higher oxidation state of sulfur (e.g. thiosulfate and sulfate) requires a higher overpotential 0.8 V vs. SCE, in the presence of perchloric acid, while in chloride medium a considerable lower overpotential is needed. Ahlberg and Asbjornsson [13] studied the galena electrochemical behaviors in acidic perchlorate media at pH 2.0, the results suggested the galena dissolution at 0.65 V and they proposed that not only elemental sulfur, but also a compound of sulfur having a greater oxidation state (e.g. thiosulfate and sulfate), are also products of the reaction depending on the potential imposed.

During the galena weathering or hydrometallurgy process, temperature and potential are common affecters. To our knowledge, no quantitative electrochemical corrosion current density, and passive/active parameters of galena under the above conditions have been reported. Therefore, in this study, a massive galena electrode electrochemical behavior was studied under different temperatures and applied potentials conditions. First, potentiodynamic polarization was used to obtain the galena corrosion current density and corrosion potential, and get the galena passive-active potential ranges. Then, EIS at different potentials correspond to the various passive/active potential ranges was performed, to understand the mechanism of galena anode at different anodic potentials that represent the difference anodic regions of potentiodynamic *i-E* curves, and further compare in what extent the temperature and potential affect the galena corrosion electrochemical parameters. These experimental results will give experimental basis for galena weathering explains and hydrometallurgy applied.

2. EXPERIMENTAL

2.1. Electrode preparation

High-quality natural galena was obtained from the Dongchuan Pb-Zn deposit of Yunnan Province, China. X-ray powder diffraction analysis confirmed that the ore sample was composed of PbS and ZnS, and electron microprobe analysis confirmed that the Pb, S and Zn contents (wt%) were 86.53%, 13.39% and 0.0064%, respectively. The galena electrode was prepared by cutting the galena

sample into approximately cubic pieces with working areas of 0.25 cm^2, avoiding visible imperfections as much as possible. After cleaning the pieces in detergent, ethanol and ultrapure water, the specimens were placed on an epoxy resin, and each was connected to a copper wire using silver paint on its back face, exposing only one face of the electrode to the solution. Prior to each test, the mineral electrode was polished with 1200$^{\#}$ carbide paper to obtain a fresh surface, degreased using alcohol, rinsed with deionized water and dried in a stream of air, the detailed electrode preparation was introduced in Jin et al previous work [14].

2.2. Electrochemical measurements

Electrochemical measurements were performed using a computer-controlled electrochemical measurement system on a conventional three-electrode electrolytic cell with platinum as an auxiliary electrode and the galena electrode as the working electrode. A saturated calomel electrode was used as a reference electrode for all of the electrochemical tests. All potentials quoted in this study are relative to the SCE (242 mV vs. standard hydrogen electrode) unless otherwise noted. The reference electrode was connected to a Luggin capillary to minimize the ohmic drop in the electrolyte. The electrolyte was pH 2.0 HNO$_3$ in order to avoid any complex formation of the generated species formed upon polarization of the electrode. The working, auxiliary and reference electrodes were placed in the same location to ensure a uniform spatial relationship.

Potentiodynamic curves were obtained by scanning the electrode potential from -250 to + 600 mV (vs. open current potential, OCP) at a scan rate of 0.5 mV·s^{-1}. EIS tests were performed at OCP and in the frequency range of 0.001~10,000 Hz with a peak-to-peak amplitude of 10 mV. Four different anodic potentials (OCP, 200, 260 and 500 mV) at low-potential (from OCP to 160 mV), mid-potential region (from 160 to 320 mV) and High-potential region (> 320 mV) were tested, respectively. ZSimpWin 3.20 (2004) software was used to fit the impedance data. To ensure reproducibility, at least three identical experiments were conducted to ensure that the reported results were reproducible (i.e., the random errors of all three identical experimental results were within tolerance), and the results reported in this study are the averages of these repetitions.

Prior to obtaining the polarization curves and conducting EIS, OCP tests were performed. During the OCP tests, the electrode potential increased for 300 s and then reached a quasi-steady state, defined here as a change of less than 2 mV per 300 s. The electrode was then stabilized for 400 s, and this potential was recorded as t2.he OCP. During the second and third replicates, if the potential was not within ± 5 mV of the value from the first test at the quasi-steady state, then the OCP test was terminated, and a new test was performed until the OCP from the first test was obtained when stabilized for 400 s [14].

3. RESULTS AND DISCUSSION

3.1 Galena potentiodynamic study

Fig. 1 shows the potentiodynamic curves for the galena electrode in pH 2.0 nitric acid solution under different temperatures at a scan rate of 0.5 mV·s^{-1}. An obvious character is with temperature

increasing, the polarization curves shift to the positive direction along the horizontal and longitudinal axes, indicating that the galena corrosion current continuous increasing, accompanying corrosion potential shift positive.
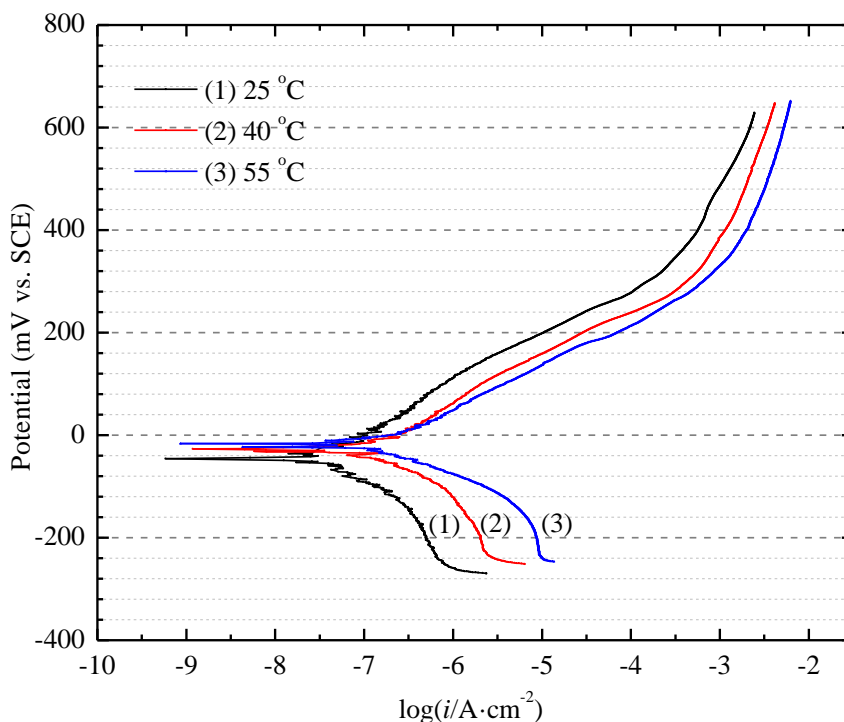
Figure 1. Potentiodynamic curves for galena in pH 2.0 HNO_3 electrolyte at a scan rate 0.5 mV·s^{-1}.

At the stronger polarization region, the corrosion potential (E_{corr}), corrosion current density (i_{corr}), Tafel slopes of anode (b_a) and cathode (b_c), were calculated according to electrochemical theory using the PAR software [15]. Besides, the polarisation resistance values, R_p, can be calculated from the Stern-Geary equation $R_p = b_a b_c / [2.3(b_a + b_c)i_{corr}]$ [16]. The polarisation experimental results are listed in Table 1.

Table 1. Electrochemical parameters of PbS under different temperatures

Temperature (°C)	E_{corr} (mV)	i_{corr} (µA·cm^{-2})	b_c (mV)	b_a (mV)	R_p (KΩ·cm^2)
25	-28.51	0.045	167.60	98.37	598.4
40	-22.42	0.15	154.34	97.81	171.9
55	-20.22	0.19	89.15	90.02	102.4

When temperature increased from 25 °C to 40 °C, the i_{corr} of the galena electrode increased from 0.045 µA·cm^{-2} to 0.15 µA·cm^{-2}, and reached 0.19 µA·cm^{-2} at 55 °C indicating that higher temperature accelerates galena corrosion, and the promotion efficiency (η) were 233.33% and

322.22%, respectively. In this study, the η is defined by $\eta\% = (i_{corr}^0 - i_{corr})/i_{corr}^0 \cdot 100\%$, which is often used at material science [17, 18]. Here, i_{corr}^0 and i_{corr} are the corrosion current density before and after the temperature change, respectively. This behavior is explained by the fact that increasing temperature causes a conversion of internal energy into electrochemical energy, decreasing the galena polarization resistance, namely, decreased from 598.4 to 171.9 and then to102.4 $\Omega \cdot cm^2$ with the temperature increased from 25 °C to 40 °C and then to 55 °C. Specifically, to the anodic and cathodic interaction, this phenomenon is explained as follows.

At the anode, galena was oxidized as Reaction (1), and S^0 is produced and can be absorbed on the galena electrode surface. Obviously, higher temperature is favorable for the oxidization of galena, which corresponds to the decrease in the galena anodic Tafel slope, that is, b_a decreased successively from 98.37 to 97.81 and 90.02 mV, when temperature increased from 25 °C to 40 °C and then to 55 °C, successively.

At the cathode, the dissolved oxygen was reduced as Reaction (2). The ionic product constant of water K_w (where $K_w = \alpha_{H^+} \cdot \alpha_{OH^-}$, $\alpha_{H^+} = \alpha_{OH^-}$ and α is activity or effective concentration.) increased with higher temperature [19], which is well known that the pH of pure water falls as the temperature increases. In other words, H^+ effective concentration (α_{H^+}) will increase with temperature increases. Obviously, bigger α_{H^+} is favorable for the reduction of O_2 according Reaction (2), resulted in the Tafel slope of cathode (b_c) decreased from 167.60 to 154.34 and 89.15 mV.

Compare the Tafel slope of anode and cathode of galena at the three different temperatures, we find that the Tafel slope changed of anode was 78.45 mV (decreased from 167.60 to 89.15 mV) was bigger than that's of cathode 8.35 mV (decreased from 98.37 to 90.02 mV) when temperature increased from 25 °C to 55 °C, meaning the interaction of cathode was dominant, that was why the corrosion potential (E_{corr}) shift to the positive direction. This result is corresponding with the polarization curve character, that is, there had a potential area that the current did not change with potential change in the cathode, revealed that the interaction is oxygen diffusion-controlled processes.

Anode: $PbS \rightarrow Pb^{2+} + S^0 + 2e^-$ (1)

Cathode: $O_2 + 4H^+ + 4e^- \rightarrow 2H_2O$ (2)
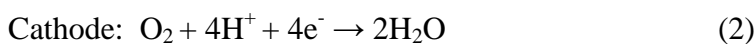
From the E-I profiles we can see three different potential ranges, OCP to ~ 160 mV, ~160 to ~ 320 mV, and above 320 mV. Relative descriptions about the three potential ranges are shown as follows.

From OCP to ~ 160 mV, there is a passive area, which could due to the formation of a thin surface layer S^0 via Reaction (1). In this study, the passive phenonmenon has appeared, but not very obviously, especially to 40 °C to 55 °C, the cause is higher temperature inhibits S^0 adhere on the electrode surface.

The rise in anodic potential can promote the oxidation sulphur to some higher oxidation state, thiosulphate, as Reaction (3) and Reaction (4). In this study, the potential range is 160 ~ 320 mV, and during this region the galena is in an active potential region. According to thermodynamic data, the Washington National Bureau of Standards [20] calculated the E^0 value of Reaction (4) was 180 mV.

$2S^0 + 3H_2O \rightarrow S_2O_3^{2-} + 6H^+ + 4e^-$ (3)

$2PbS + 3H_2O \rightarrow PbS_2O_3 + Pb^{2+} + 6H^+ + 8e^-$ (4)
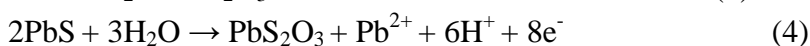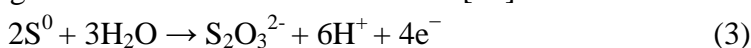
When the anodic potential was above 320 mV, the *i-E* curve slope had another obviously changed, indicating another anodic reaction occur, namely, $S_2O_3^{2-}$ changed into SO_4^{2-} as Reaction (5) shown [11]:

$$S_2O_3^{2-} + 5H_2O \rightarrow 2SO_4^{2-} + 10H^+ + 8e^- \qquad (5)$$

3.2 Electrochemical impedance spectroscopy study

EIS has been widely applied for studying the characteristics of electrodes and electrochemical reactions [21]. In this section, EIS studies were used to confirm the previous polarization curves, and clarify the mechanism of electrochemical oxidation of the galena.

3.2.1 Low-potential region (OCP to 160 mV)
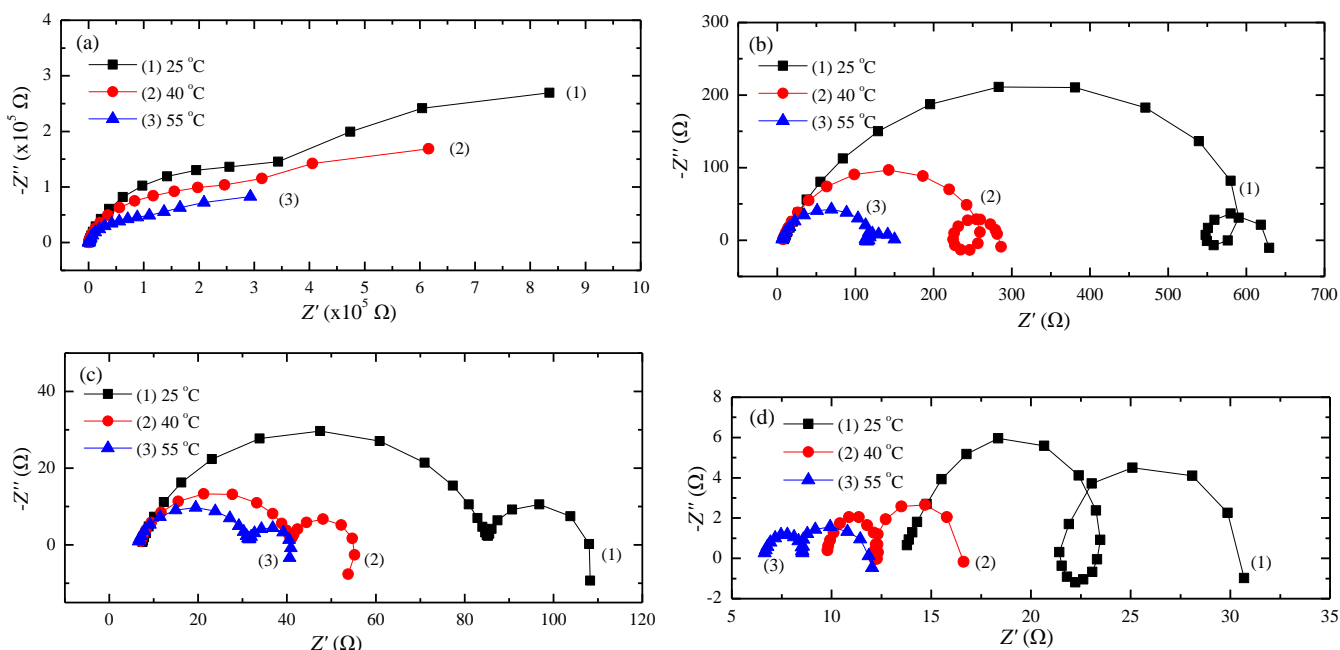
Figure 2. Nyquist plots of the galena electrode under different temperatures at OCP (a), 200 mV (b), 260 mV (c), and 500 mV (d). Conditions: pH 2.0, temperature (1) 25, (2) 40 and (3) 55 °C.

Fig. 2 (a) and Fig. 3 (a) present the Nyquist and Bode plots for galena at OCP under pH 2.0 nitric acid solution, respectively. The Nyquist plots are composed of two capacitive loops, the one at high frequencies is attributed to the charge transfer resistance (R_t), which could correspond to the resistance between the galena and the outer Helmholtz plane, and the other slightly distorted capacitive loop at low frequencies is related to the combination of a pseudo-capacitance impedance (due to the passive layer) and a resistance R_p.
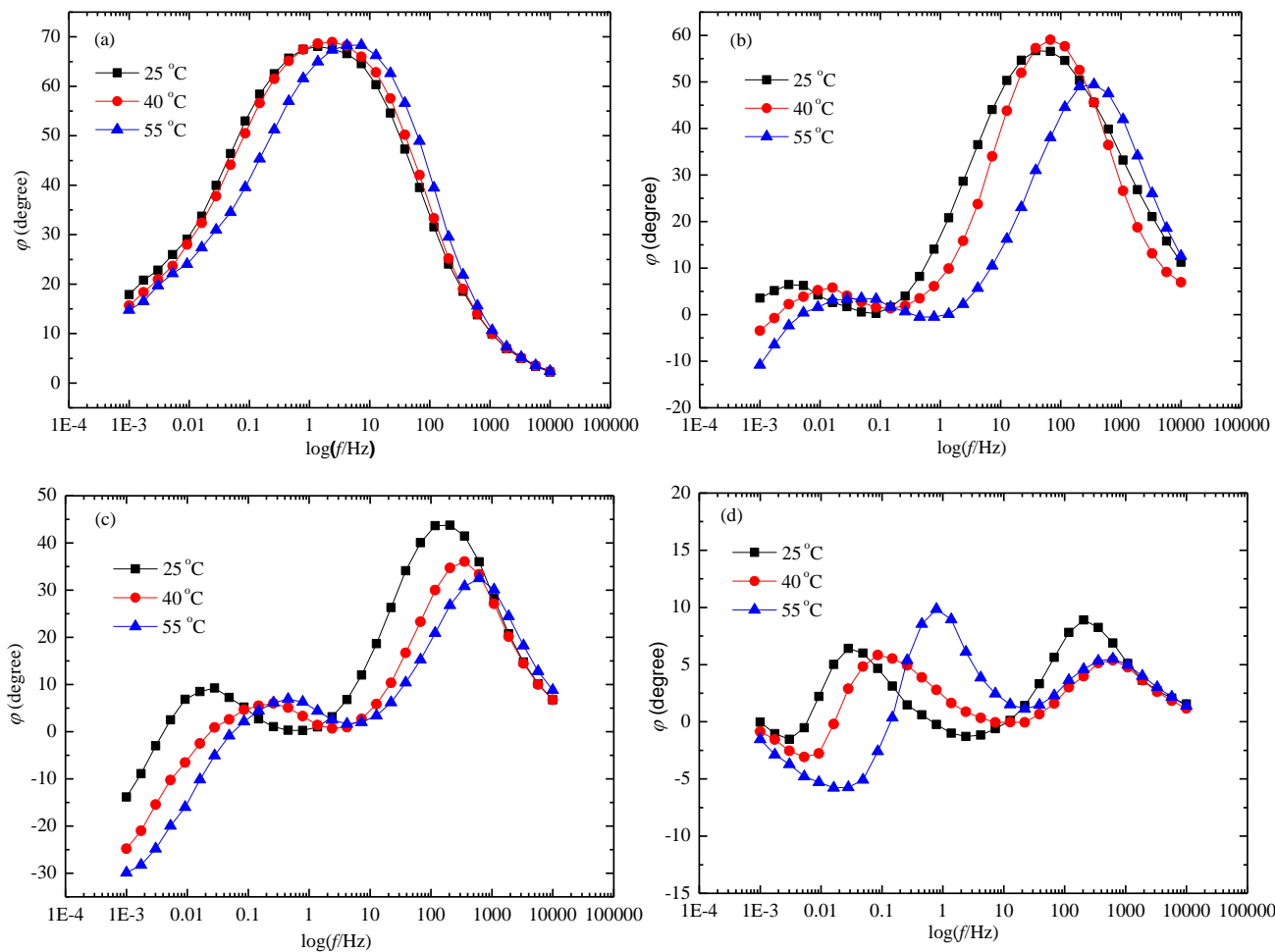
Figure 3. Bode plots of the galena electrode under different temperatures at OCP (a), 200 mV (b), 260 mV (c), and 500 mV (d). Conditions: pH 2.0, temperature (1) 25, (2) 40 and (3) 55 °C.
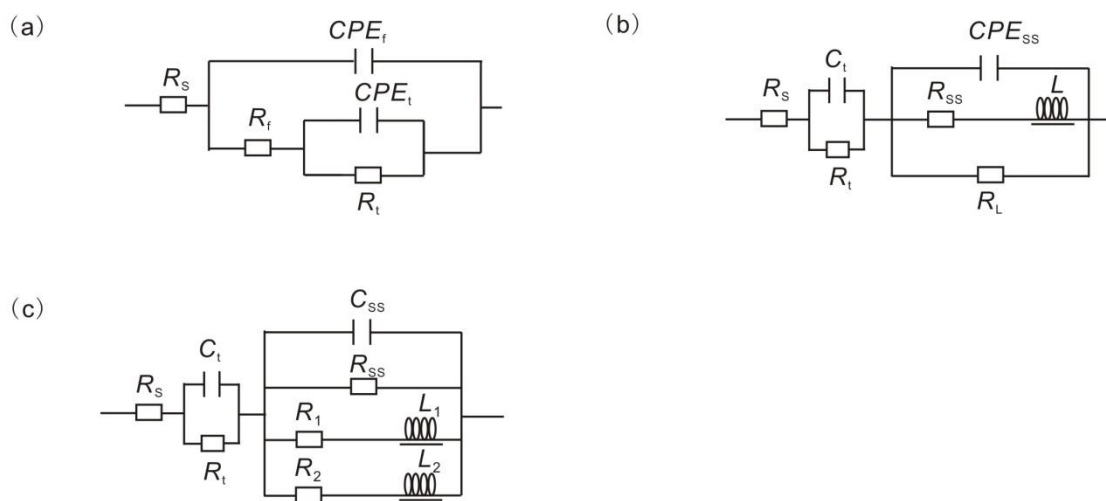
Figure 4. Equivalent circuit for the galena electrode/electrolyte at OCP (a), 200 and 260 mV (b), and 500 mV (c).

　　　The deviation from an ideal semicircle is generally attributed to the frequency dispersion as well as to the in-homogeneities of the passive layer surface. The related electrochemical equivalent circuit (EEC) used to model the galena/electrolyte interface is shown in Fig. 4 (a), where R_s is the solution resistance, R_t is the charge transfer resistance, R_p is the passive film resistance, CPE_t and CPE_p represent constant phase element to replace the charge transfer capacitance at the double layer (C_t), and passive film capacitance (C_p), respectively. Constantin and Chirita [22] and Ouyang et al. [23] have used this model to explain the oxidative dissolution of pyrite in acidic media, and Pang et al. [24] provided a detailed theoretical explanation of this EEC model. Because the equivalent circuits represent an approach to describe the electrochemical processes that occur at the electrode/electrolyte interface, any models derived from them are only tentative [25]. For this reason, different EECs were used to fit the EIS data, and only those results with the best fitting values capable of efficiently explaining the electrode/electrolyte interface were reported. The impedance parameters obtained by fitting the EIS data to the equivalent circuit are listed in Table 2.

Table 2. Model parameters for equivalent circuit of Fig. 3 (a) at OCP

Temperature (°C)	CPE_t, Y_0 (S·cm^{-2}·s^{-n})	n	R_t (Ω·cm^2)	CPE_p, Y_0 (S·cm^{-2}·s^{-n})	n	R_p (Ω·cm^2)
25	4.276×10^{-5}	0.8085	7.182×10^{4}	4.354×10^{-4}	0.9622	1.103×10^{5}
40	6.102×10^{-5}	0.8012	5.274×10^{4}	5.699×10^{-4}	0.8042	5.824×10^{4}
55	6.644×10^{-5}	0.7955	3.689×10^{3}	7.288×10^{-4}	0.5236	1.077×10^{4}

　　　The results show that the double layer charge transfer resistance decreased from 7.182×10^{4} to 3.689×10^{3} Ω·cm^2 and the capacitance parameter CPE_t, Y_0 increased from 4.276×10^{-5} to 6.644×10^{-5} S·cm^{-2}·s^{-n} with the temperature increased from 25 °C to 55 °C, suggesting that charge transfer was facilitated at the double layer. For the galena passive film, increased temperature from 25 °C to 55 °C caused the passive resistance decreased from 1.103×10^{5} to 1.077×10^{4} Ω·cm^2 and the capacitance parameter CPE_t, Y_0 increased from 4.354×10^{-4} to 7.288×10^{-4} S·cm^{-2}·s^{-n}. To the parameter n, it is a value representing the deviation from purely capacitive behavior. When the value of n approaches unity, pure capacitive behavior is observed [26] When n < 1, the system shows a behavior that has been attributed to surface heterogeneity [27] or to continuously distributed time constants for the charge transfer reactions [25, 28, 29]. In this study, with the temperature increasing from 25 °C to 40 °C and then to 55 °C, the passive film exponent n values decreased from 0.9622 to 0.8042 and then to 0.5236, confirming that the degree of passive surface inhomogeneity increased with increasing temperature. Especially, when electrolyte is 55 °C, the value of n near 0.5 (Warburg diffusion) indicates that the galena electrode is in concentration polarization, and the limiting step may be a diffusion process, meaning defects in the passive film appear, and explaining the observed decrease of the charge transfer resistance with temperature. In a word, smaller resistance of charge transfer between double layer and of the film, and larger capacitance of double layer and of the film, indicate galena charge transfer changed easier and passive film changed weakness. All of these results are agree with the polarization curves results, namely, higher temperature prove galena electrochemical dissolution at OCP [14].

3.2.2 Mid-potential region (from 160 to 320 mV)

Fig. 2 (b, c) and Fig. 3 (b, c) show the Nyquist and Bode plots for the galena at the anodic potential 200 mV and 260 mV, respectively. Two time constants were clearly observed from the Nyquist and Bode plots. The high frequency impedance loop is the result of charge transfer resistance and double-layer capacitance coupling. The mid-frequency impedance loop and low frequency inductive impedance loop are characteristic of anodic dissolution of semiconductor electrodes [30, 31]. In this potential range, electrochemically active dissolution of the electrode occurs and none of the passive layers formed at lower potentials is stable. EEC shown in Fig. 4 (b) was employed to fit the experimental data, Ghahremaninezhad et al. [32] have used it for galena electrochemical parameters simulate at this active potential area. Where, the C_t/R_t pair represents the charge transform capacitive and resistive behavior in the double layer region, respectively. The $CPE_{ss}\|R_L\|(LR_{SS})$ section of the model represents the dissolution of semiconductor electrodes in which CPE_{SS} and R_{SS} contribute to the surface states on electrode, R_L corresponds to the resistance associated to the accumulation of superficial species and the element L is an equivalent inductance that indicates the on-going reaction process (Reaction (3)). The values of the different elements in the equivalent circuit of 200 and 260 mV are shown in Table 3 and Table 4, respectively.

Table 3. Model parameters for equivalent circuit of Fig. 3 (b) at 200 mV

Temperature (°C)	C_t (F·cm^{-2})	R_t (Ω·cm^2)	CPE_{ss} (S·cm^{-2}·s^{-n})	n	R_{ss} (Ω·cm^2)	L (H·cm^{-2})	R_L (Ω·cm^2)
25	0.7267	86.63	1.507×10^{-4}	0.7681	3770	4268	666.5
40	0.3918	59.91	1.142×10^{-4}	0.8092	1663	843.4	257.0
55	0.2078	55.86	8.460×10^{-5}	0.8154	18.50	420.4	117.4

At the potential of 200 mV (Table 3), we can see: (1) at an arbitrary same temperature (25 °C, 40 °C or 55 °C), compare to the results at OCP, the charge transfer resistance R_t value had a dramatic decrease, that is, decreased from 7.182×10^4 to 86.63 Ω·cm^2, 5.274×10^4 to 59.91 Ω·cm^2 and 3.689×10^3 to 55.86 Ω·cm^2 at 25 °C, 40 °C and 55 °C, respectively. All of these data are well corresponding with previous potentiodynamic curves results, that is, the galena electrode suffered from passive stage changed into active stage, and the passive surface completely dissolute, which is very helpful charge transfer. (2) to the double layer, the galena charge transfer resistance decreased from 86.63 to 59.91 Ω·cm^2, and then decreased to 55.86 Ω·cm^2, when electrolyte temperature increased from 25 °C to 40 °C and then to 55 °C, respectively, confirmed that high temperature accelerate the galena electrochemical dissolution; furthermore, the double layer capacitance decreased with temperature increased, according to Gouy-chapman double layer model [33], the cause is due to the particle motion rate increased with the temperature increase, and resulted in the thickness of diffuse layer spread, leading to local ions concentration decreased. (3) As to the parameters of the surface states on electrode, R_{SS} decreased, meaning the galena semiconductor electrode dissolution resistance decrease with the temperature decreased, meanwhile, CPE_{SS} also decreased followed exponent n values increased (revealing surface homogeneity/area increased, local ions concentration decreased) with

increasing temperature. Furthermore, parameter R_L decreased from 666.5 to 257.0 $\Omega \cdot cm^2$, and then to 117.4 $\Omega \cdot cm^2$, accompanied with equivalent L value dropped from 4268 to 843.4 $H \cdot cm^{-2}$, and then to 420.4 $H \cdot cm^{-2}$, respectively. A lower accumulation resistance value of R_L and lower transfer inductance L indicate chemicals are difficult to accumulate on the superficial film and could easily cross the double layer, which reveals that the temperature improved the galena electrode electrochemical dissolution.

When potential reached to 260 mV, the model parameters (Table (4)) changed trend were similar to that of 200 mV. Higher temperature resulted lower values of R_t and C_t at double layer, smaller values of R_{SS} and CPE_{SS} related surface states on electrode, and smaller values of the accumulation of superficial species R_L and L.

Table 4. Model parameters for equivalent circuit of Fig. 3 (b) at 260 mV

Temperature (°C)	C_t (F·cm^{-2})	R_t (Ω·cm^2)	CPE_{ss} (S·cm^{-2}·s^{-n})	n	R_{ss} (Ω·cm^2)	L (H·cm^{-2})	R_L (Ω·cm^2)
25	0.2862	27.04	1.138×10^{-4}	0.8126	585.6	6129	87.04
40	0.1020	16.13	9.521×10^{-5}	0.8479	25.5	2048	36.60
55	0.0536	12.02	8.088×10^{-5}	0.8527	12.36	616.5	25.62

Table 5. Model parameters for equivalent circuit of Fig. 3 (c) at 500 mV

Temperature (°C)	C_t (F·cm^{-2})	R_t (Ω·cm^2)	C_{ss} (F·cm^{-2})	R_{ss} (Ω·cm^2)	R_1 (Ω·cm^2)	L_1 (H·cm^{-2})	R_2 (Ω·cm^2)	L_2 (H·cm^{-2})
25	0.3193	26.35	0.3799	23.06	118.5	5441	108.3	5180
40	0.1086	18.60	0.1181	13.67	6.635	1805	17.09	1476
55	0.0115	10.40	0.0127	9.782	3.977	406.6	7.269	267.3

Contrast to the results of 200 mV and 260 mV, more information from Table 3 and Table 4 show: at the same temperature of 25 °C, 40 °C or 55 °C, all the resistance parameters R_t, R_{SS} and R_L values decreased with the potential increased, suggesting that higher positive potential benefits the chemicals crossing the double layer and disadvantage of the accumulation of superficial species. Besides, both the equivalent inductance L and bigger exponent n values increased with potential increasing revealed more intermediate ($S_2O_3^{2-}$) produced and the electrode surface homogeneity increased. All of these data are well corresponding with previous potentiodynamic curves results, that is, the galena electrode electrochemical dissolution increases with potential increasing.

3.2.3 High-potential region (> 320 mV)

Fig. 2 (d) and Fig. 3 (d) show the Nyquist and Bode plots for the galena electrode at the anodic potential 500 mV, respectively. Compare to the plots at 200 or 260 mV, three time constants occurred, that is, a new small inductance loop, while not capacitive loop occurs at the low frequency region. This phenomenon shows there should be another product occur and this product does not accumulate on the surface, which corresponding with $S_2O_3^{2-}$ ions change into SO_4^{2-} as the above potentiodynamic curves described.

Fig. 3 (c) shows the model applied for the 500 mV Nyquist plots, where, the C_t/R_t pair represents the charge transform capacitive and resistive behavior in the double layer, respectively. The $C_{ss}||R_{ss}||(L_1R_1)$ section of the model represents the dissolution of semiconductor electrodes in which C_{SS} and R_{SS} contribute to the surface (or interface) states on electrode, R_1 corresponds to the resistance associated to the accumulation of $S_2O_3^{2-}$ ions and the element L_1 is an equivalent inductance corresponds to the $S_2O_3^{2-}$ ions relax process. The $L_2||R_2$ section of the model represents the SO_4^{2-} ions relax process, R_2 corresponds to the resistance associated to the accumulation of SO_4^{2-} ions and the element L_2 is an equivalent inductance corresponds to the SO_4^{2-} ions relax process. The values of the different elements in the equivalent circuit are shown in Table 5.

From the Table 5 we can see: (1) electrochemical parameters R_t and R_{SS} were all decreased with the electrolyte temperature increased, revealing higher temperature favorable for charge transfer at the double layer and advantage of galena semiconductor electrode dissolution. (2) ions accumulation resistance R_1, R_2 and relax process inductance L_1 , L_2 of $S_2O_3^{2-}$ and SO_4^{2-} were all decreased, suggesting $S_2O_3^{2-}$ and SO_4^{2-} ions were difficult to accumulate on the superficial film and could their relax progress changed faster with electrolyte temperature increased.

4. IMPLICATIONS

As one of the most affect factor, temperature greatly affects galena weathering in Pb-Zn mine at different temperature regions or seasons. In hydrometallurgy, select an appropriate temperature is often taken as important method to improve hydrometallurgy rate. This study confirmed that higher temperature accelerate galena dissolution, especially, galena electrochemical dissolution promotion efficiency reached 233.33% when temperature increased from 25 °C to 40 °C, and was 322.22% from 25 °C to 55 °C. The results suggest, considering production cost and equipment requirement, in real galena hydrometallurgy, select a slightly above room temperature (such as 40 °C) whereas not higher temperature (such as 55 °C) is appropriate. Though previous papers had not quantitative data to discover the promotion efficiency related increase temperature, however, Many researchers [28,] have revealed that temperature is an important factor affects (bio) leaching of sulfide minerals

In galena hydrometallurgy progress, galena will be passive at OCP and thus inhibit galena electrochemical dissolution. This study revealing increases potential to about 160 ~ 320 mV can drop galena into active status when galena is in HNO_3 at pH 2.0, accelerating galena electrochemical dissolution. Note to pointed out the critical potential is different for galena transfer into thiosulfate and sulfate when galena in different electrolyte media, such as, it is 0.6 V vs SCE in perchlorate medium at

pH 0 [11], 0.54 V vs SCE in perchlorate medium at pH 2.0 [12], and 0.65 V in acidic perchlorate media at pH 2.0. So, apply an appropriate potential to active galena is another an important method to improve hydrometallurgy rate.

5. CONCLUSIONS

The electrochemical dissolution behaves of galena in pH 2.0 HNO_3 under different temperatures and potentials were investigated by potentiodynamic polarization, electrochemical impedance spectroscopy. Based on the established electrochemical parameters of galena, the following conclusions could be derived:

(1) Galena electrochemical oxidizes presence of different electrochemical reaction states and electrode surface characters. From OCP to 160 mV was passive area, where a thin surface layer S occurred; 160-320 mV was active area, surface layer S^0 changed into $S_2O_3^{2-}$; and when potential above 320 mV was double-inductive area, $S_2O_3^{2-}$ transformed into SO_4^{2-}.

(2) High temperature causes galena corrosion potential shift to the positive direction, accelerates galena electrochemical dissolution, and the promotion efficiency are 233.33% and 322.22%, respectively, when temperature increases from 25 °C to 40 °C, and then to 55 °C.

(3) EIS results are well with the three potential regions, and reveal the cause that high temperature accelerates galena electrochemical due to decreases charge transform resistance and passive resistance at passive potential area; at active potential area (160-320 mV), S change into $S_2O_3^{2-}$, and change into SO_4^{2-} at higher potential.

References

1. J. Ralston, *Miner. Eng.,* 7 (1994) 715.
2. T. Fang, G. J. Liu, C. C. Zhou, R. Y. Sun, J. Chen and D. Wu, *Environ. Geochem. Health*, 36 (2014) 563.
3. S. G. Salamy and J. G. Nixon, The application of electrochemical methods to flotation research. In: Recent developments in mineral dressing, (1953) London: Institution of Mining and Metallurgy.
4. A. N. Buckley and R. Woods, *Appl. Surf. Sci.*, 17 (1984) 401.
5. K. Laajalehto, R. S. C. Smart, J. Ralston and E. Suoninen, *Appl. Surf. Sci.*, 64 (1993) 29.
6. P. E. Richardson, R. H. Yoon and R. Woods, *Int. J. Miner. Process*, 41 (1994) 77.
7. J. B. Brodie, The Electrochemical Dissolution of Galena. M.Sc. Thesis, (1969) University of British Columbia.
8. G. W. Poling and J. Leja, *J. Phys. Chem.*, 67 (1963) 2121.
9. R. G. Greenler, *J. Phys. Chem.*, 66 (1962) 879.
10. A. S. Manocha and R. L. Park, *Appl. Surf. Sci.*, 1 (1977) 129.
11. J. L. Nava, M. T. Oropeza and I. González, *Electrochim. Acta*, 47 (2002) 1513.

12. I. C. González, M. T. Oropeza-Guzmán and I. González, *Electrochim. Acta*, 45 (2000) 2729.
13. E. Ahlberg and J. Asbjornsson, *Hydrometallurgy*, 34 (1993) 171.
14. G. H. Jin, L. Y. Wang, K. Zheng, H. P. Li and Q. Y. Liu, *Ionics*, 22 (2016) 975.
15. A. G. Bard and L. T. Faulkner, Electrochemical methods: fundamentals and applications, 2nd. Hoboken: Wiley and Sons. Angew Chem Int Edit 41(2000) 655.
16. M. Stern and A. L.Geary, *J. Electrochem. Soc.*, 104 (1957) 56.
17. R. Solmaz, G. Kardaş, B. Yazici and M. Erbil, *Colloids Surf. A.*, 312 (2008) 7.
18. X. Wang, H. Yang and F. Wang, *Corros. Sci.*, 53 (2011) 113.
19. W. L. Marshall and E. U. Frank, *J. Phys. Chem. Ref. Data*, 10 (1981) 295.
20. D. D. Wagman, W. H. Evans, V. B. Parker, I. HaIow, S. M. Bailey and R. H. Schum, Selected Values of Chemical Thermodynamic Properties, Washington National Bureau of Standards, Technical Note. 51 (1965) 65.
21. M. E. Orazem, B. Tribollet, *Electrochim. Acta*, 53 (2008) 7360.
22. C. A. Constantin and P. Chirita, *J. Appl. Electrochem.*, 43 (2013) 659.
23. Y. H. Ouyang, Y. Liu, R. L. Zhu, F. Ge, T. Y. Xu, Z. Luo and L. B. Liang, *Miner. Eng.*, 72 (2015) 57.
24. J. Pang, A. Briceno and S. Chander, *J. Electrochem. Soc.*, 137 (1990) 3447.
25. J. R. Macdonald, *J. Appl. Phys.*, 58 (1985) 1971.
26. K. S. Cole and R. H. Cole, *J. Chem. Phys.*, 9 (1941) 341.
27. G. J. Brug, A. L. G. Vandeneeden, M. Sluytersrehbach and J. H. Sluyters, *J. Electroanal. Chem.*, 176 (1984) 275.
28. Z. Lukacs, *J. Electroanal. Chem.*, 464 (1999) 68.
29. J. R. MacDonald, *J. Appl. Phys.*, 58 (1985) 1955.
30. B. H. Erne and D. Vanmaekelbergh, *J. Electrochem. Soc.*, 144 (1991) 3385.
31. W. P. Gomes and D. Vanmaekelbergh, *Electrochim. Acta*, 41 (1996) 967.
32. A. Ghahremaninezhad, E. Asselin and D. G. Dixon, *Electrochim. Acta*, 55 (2010) 5041.
33. G. H. Bolt, *J. Colloid Sci.*, 10 (1995) 206.
34. B. Escobar, S. Buccicardi, G. Morales and J. Wiertz, *Hydrometallurgy*, 104 (2010) 454.
35. A. Iliyas, K. Hawboldt and F. Khan, *J. Hazard. Material.*, 2010,178 (2019) 814.